Int. J. Electrochem. Sci., 10 **(2015)** 2306 - 2323

International Journal of
ELECTROCHEMICAL
SCIENCE
www.electrochemsci.org

Synthesis, Spectroscopic, Physicochemical, Crystal Structure and DFT Studies of 4,5,6,7-tetrahydro-1-benzothiophene-3-carbonitrile Based Azomethine Dyes

Salman A. Khan[1,*], *Abdullah Y. Obaid*[1], *Laila Mohammad Al-Harb* [1], *Muhammad Nadeem Arshad*[1,2], *Abdullah M. Asiri*[1,2], *Michael B. Hursthouse*[3]

[1] Chemistry Department, Faculty of Science, King Abdulaziz University P. O. Box 80203, Jeddah 21589, Saudi Arabia
[2] Centre of Excellence for Advanced Materials Research (CEAMR), King Abdulaziz University P. O. Box 80203, Jeddah 21589, Saudi Arabia
[3] School of Chemistry, University of Southampton, Southampton, SO17 1BJ, UK
[*]E-mail: sahmad_phd@yahoo.co.in

Received: 14 September 2014 / *Accepted:* 25 December 2014 / *Published:* 19 January 2015

Three new azomethine dyes were synthesized via a simple condensation method using 2-amino-4,5,6,7-tetrahydro-benzo[b]thiophene-3-carbonitrile and a variety of aldehydes. The structures of synthesized compounds were established by spectroscopic (FT-IR, ^{1}H NMR, ^{13}C NMR, MS) and elemental analyses. UV-Vis and fluorescence spectroscopy measurements proved that all compounds have good absorbance and fluorescence properties. Fluorescence polarity studies demonstrated that these compounds were sensitive to the polarity of the microenvironment provided by different solvents. In addition, spectroscopic and physicochemical parameters, including singlet absorption, extinction coefficient, Stokes shift, oscillator strength and dipole moment, were investigated in order to explore the analytical potential of the synthesized compounds. Three-dimensional structures were studied using single crystal x-ray diffraction. Optimized geometries, electronic structure and frontier molecular orbital energies were studied theoretically, and the energy gap (ΔE) of II was found to be relatively greater than those for I and III, while I and III have almost the same energy gaps.

Keywords: Schiff base; Physicochemical; X-ray; Theoretical calculations

1. INTRODUCTION

Azomethine compounds (R-N=C-R') are generally synthesized by the condensation of primary amines with carbonyl compounds [1]. They are also known as Schiff bases, due to the presence of a lone pair of electrons in an *sp*^{2}-hybridized orbital of the nitrogen atom of the azomethine group, which makes them chemically and biologically important compounds [2]. They are used an intermediates for the formation of various heterocyclic compounds such as oxazoles, thiadiazolines, thiazolidones [3, 4]. Schiff bases have been used as ligands for the formation of metal complexes such as with Cu(II), Ni(II), Co(II), Pd(II), Pt(II) [5]. These complexes are relevant for bioinorganic chemistry, biomedical applications, supramolecular chemistry and catalysis [6-9]. On the other hand, a large number of different Schiff base derivatives have been used in the field of materials science like solar shell [10], optical switching [11], third order non-linear optics (NLO) [12], electrochemical sensing [13], Langmuir films and photo-initiated polymerization [14], They are well known for their biological application as antibacterial [15], antifungal, antiviral, anti-HIV [16], anti-protozoal [17], anti-cancer agents [18]. Because of these numerous applications of Schiff bases derivatives, we are reporting here the synthesis of some novel heterocyclic compounds, their single crystal X-ray studies and density functional theory (DFT) calculations. Physicochemical studies such as electronic absorption, molar absorptivity, oscillator strength and dipole moment are also reported

2. EXPERIMENTAL

2.1. Materials and Methods

All the chemicals and solvents were purchased from Merck (Germany) and Aldrich (U.S.A.). Melting points were determined on a Stuart-SMP10 melting point apparatus using open-glass capillaries and are reported as uncorrected. IR absorption spectra were recorded on a Shimadzu FTIR-8400s using KBr pellets in the 4,000–400 cm-1 range. ^{1}H-NMR and ^{13}C-NMR spectra were recorded on a Bruker-AVANCE-III 600 MHz spectrophotometer. The values are reported in term of chemical shifts as parts per million (ppm) downfield taking TMS (Me_4Si) as an internal standard. The splitting patterns are designated as follows; s, singlet; d, doublet; m, multiplet. Mass spectra were recorded on a EI-MS spectrometer. 2-amino-4,5,6,7-tetrahydro-benzo[b]thiophene-3-carbonitrile was prepared by the published method [19].

2.2. General procedure for the synthesis of Schiff Bases

A mixture of 2-amino-4,5,6,7-tetrahydro-benzo[b]thiophene-3-carbonitrile (5.8 mmol) and corresponding active aldehyde (5.8 mmol) in anhydrous methanol (15 ml), was refluxed at 80 ºC for 3 h with continuous stirring in the presence of few drop of acetic acid. Progress of the reaction was monitored by TLC [20]. After completion of the reaction the solution was cooled. The heavy precipitate thus obtained was collected by filtration and recrystallization from methanol and chloroform gave (1-3) (Scheme 1).

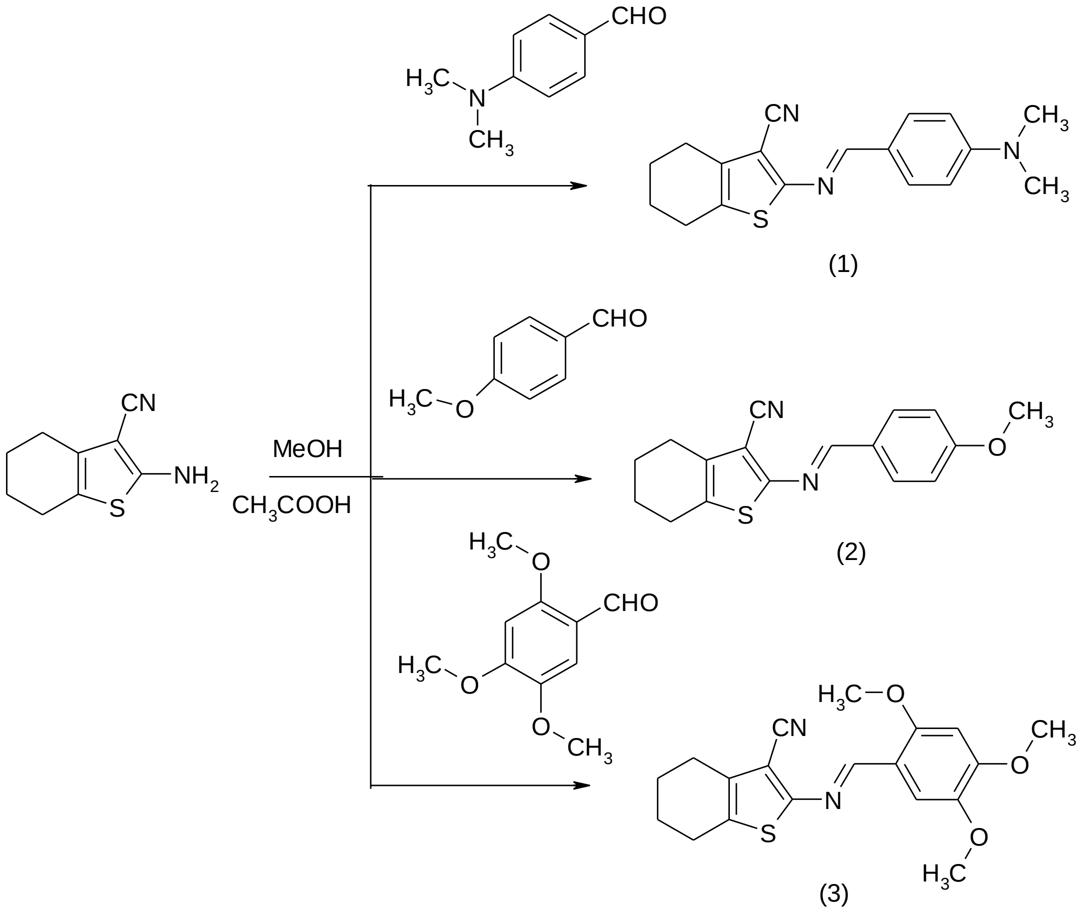

Scheme 1. Synthesis of targeted molecules **(1-3)**

2.3. 2-[4-(dimethylamino)phenylmethylidene)amino]-4,5,6,7-tetrahydro-1-benzothiophene-3-carbonitrile (1)

FT-IR (KBr) ν_{max} cm^{-1}: 2914 (C-H), 1625 (C=C), 1560 (C=N), 1167 (C-N); ^{1}H-NMR ($CDCl_3$) δ: 9.75 (s, 1H, CH$_{olefinic}$), 8.29 (d, CH$_{aromatic}$, *J* = 7.6 Hz), 7.86 (d, CH$_{aromatic}$, *J* = 7.8 Hz), 7.75 (d, CH$_{aromatic}$, *J* = 9.0 Hz), 6.37 (d. CH$_{aromatic}$, *J* = 9 Hz), 2.70-1.82 (m, 8H, -CH_2-), 3.10 (s, N-CH_3), 3.07 (s, N-CH_3); ^{13}C-NMR ($CDCl_3$) δ: 190.39, 158.56, 134.65, 133.86, 131.89, 130.71, 115.10, 112.58, 111.12, 104.34, 43.39, 40.78, 25.25, 25.47, 23.11, 22.89, 22.11, 5.16; EI-MS (*m/z*, %): 311 (M+1, 68); Anal. Calc. for $C_{18}H_{19}N_3S$: C, 69.87; H, 6.19; N, 13.58, Found: C, 69.82; H, 6.11; N, 13.53.

2.4. 2-{[(E)-(4-methoxyphenyl)methylidene]amino}-4,5,6,7-tetrahydro-1-benzothiophene-3-carbonitrile (2):

IR (KBr) ν_{max} cm^{-1}: 2936(C-H), 1594(C=C), 1558 (C=N), 1135(C-N), 771(C-S); ^{1}H NMR ($CDCl_3$) δ: 8.34 (s, 1H, CH$_{olefinic}$), 7.89 (d, CH, J= 6.6 Hz), 7.88 (d, CH, J= 6.2 Hz), 6.98 (d, CH, J= 6.8 Hz), 1.899-1.82 (m, 8H –CH_2), 2.60 (s, -OCH_3); ^{13}CNMR ($CDCl_3$) δ: 163.09, 160.61, 158.39, 134.84, 131.50, 131.39, 127.97, 114.78, 114.36, 105.88, 58.46, 55.51, 25.16, 24.28, 23.08, 22.01, 18.42; EI-MS m/z (rel. int.%): 298 (65) $[M+1]^{+\cdot}$; Anal. calc. for $C_{17}H_{16}N_2OS$: C, 68.89, H, 5.44, N, 9.45, Found: C, 68.84, H, 5.41, N, 9.39.

2.4. 2-{[(E)-(2,4,5-trimethoxyphenyl)methylidene]amino}-4,5,6,7-tetrahydro-1-benzothiophene-3-carbonitrile (3)

IR (KBr) v_{max} cm^{-1}: 2932(C-H), 1586(C=C), 1562 (C=N), 1127(C-N), 759 (C-S); ^1H NMR ($CDCl_3$) δ: 8.77 (s, CHolefinic), 7.70 (s, CH), 6.47 (s, CH), 3.96 (s, OCH_3), 3.94 (s, OCH_3), 3.90 (s, -OCH_3), 2.69-1.83 (m, 8H, -CH_2-cyclic); ^{13}CNMR ($CDCl_3$) δ: 161.86, 156.16, 154.45, 15.27, 143.72, 134.68, 130.95, 115.52, 114.97, 108.97, 105.09, 95.83, 58.47, 56.32, 56.26, 56.10, 25.15, 28.47, 56.32, 56.26, 56.10, 25.15, 24.30, 23.12, 22.05, 18.43; EI-MS m/z (rel. int.%): 358(62) $[M+1]^{+\cdot}$; Anal. calc. for $C_{19}H_{20}N_2O_3S$: C, 64.02, H, 5.66, N, 7.86, Found: C, 63.98, H, 5.62, N, 7.83.

2.5. Crystallography

Suitable crystals of all three compounds were selected for single crystal diffraction studies and mounted on an Agilent SuperNova Atlas Dual Source, Agilent Technologies diffractometer. The CrysAlisPro software [21] was used for data collection keeping the temperature at 296.00 K during the process. Using Xseed [22], the structure was solved with the ShelXS [23] structure solution program using Direct Methods and refined with the ShelXL refinement package using Least Squares minimization. All the hydrogen atoms were positioned with idealized geometry with where $dC_{aromatic}$-H = 0.93 Å, $dC_{methylene}$-H = 0.98 Å & dC_{methyl}-H = 0.96 Å. These were refined using a riding model with $U_{iso}(H) = 1.5\ U_{eq}(C)$ for methyl and $U_{iso}(H) = 1.2\ U_{eq}(C)$ for all other carbon atoms. The figures were drawn with the help of PLATON [24] within WinGX.[25] The crystal data were deposited at the Cambridge Crystallographic Data Centre and have been assigned the deposition numbers CCDC 959975-959977. This data can be obtained free of charge from The Cambridge Crystallographic Data Centre via www.ccdc.cam.ac.uk/data_request/cif.

2.6. Computational Methods

The computational calculation of molecules was performed using Spartan'04 Version 1.0.3 [26], with density functional theory, DFT/6-31G*basis set. The density encoded with electrostatic potential, the HOMO, and the LUMO were also studied.

3. RESULTS AND DISCUSSION

3.1. Chemistry

The synthesis of Schiff base derivatives is straightforward and the compounds were isolated in good yield. The derivatives were synthesized by using the literature procedure [27]. The obtained compounds are stable in the solid state as well as in the solution state. The analytical data of these compounds are in good agreement with their composition. The structure of all the compounds presented in experimental section was established by comparing spectral data (FT-IR, ^{1}H NMR, ^{13}C NMR, EI-Mass) and elemental analyses. Assignments of selected characteristic IR band positions provide significant indication for the formation of the Schiff base derivative. The compounds showed intense bands at 1558-1562 cm^{-1} due to v (C=N) stretch, which confirm the formation of donor-acceptor derivatives. Further evidence for the formation of Schiff base derivative was obtained from the ^{1}H-NMR spectra, which provide diagnostic tools for the positional elucidation of the protons. Assignments of the signals are based on the chemical shifts and intensity patterns. The aromatic protons of Schiff base are shown as s, d and dd in the range (6.37-7.89) ppm for the compounds. A singlet due to 1H, CH olefinic proton in the compounds was observed at (8.29-8.77) ppm respectively.

^{13}C NMR ($CDCl_3$) spectra of schiff base derivatives were recorded in $CDCl_3$ and spectral signals are in good agreement with the probable structures. Details of ^{13}CNMR spectra of all compounds are given in the experimental section. Finally characteristic peaks were observed in the mass spectra of Schiff base for the molecular ion. The mass spectra of compounds 1 2 and 3 shows a molecular ion peak ($M^{+\cdot}$) m/z 311, 298 and 358

3.2. Spectral behaviour of 4,5,6,7-tetrahydro-1-benzothiophene-3-carbonitrile Based Schiff Base Derivatives in different media

Absorption and emission spectra of 1 x10^{-5} mol dm^{-3} solutions of the compounds (1-3) in various non-polar, polar aprotic and protic solvents were studied (Fig 1a to Fig 3b). Calculated physicochemical parameters obtained from steady state absorption and fluorescence spectra are tabulated in Table 1-3. A close examination of Fig 1a-3a displays that the polarity of solvent has a little effect on absorption maxima, indicating the weak polar character of compounds (1-3) in the ground state. However, the emission spectra of these compounds are slightly red shifted as the solvent polarity increases, as shown in Fig 1b-3b. The red-shift in n-Heptane to DMF indicates that the small change in the polarity of the excited state is slightly increased than that in ground state [28]. As the result the polarity of solvents are slightly different to compounds (1-3)

Table 1. Spectral data of compound no. 1 in different solvents

Solvent	**Δf**	**E_T (30) Kcal mol^{-1}**	**λ_{ab}(nm)**	**λ_{em}(nm)**	**ε M^{-1}cm^{-1}**	**f**	**μ Debye**	**$\Delta\bar{\nu}$ (cm^{-1})**
DMF	0.275	64.53	443	489	43300	0.36	5.80	**2124**
MeOH	0.309	65.72	435	505	44200	0.40	6.07	**2290**

PrOH	0.280	65.87	434	487	28600	0.28	5.07	**2508**
ButOH	0.264	65.42	437	488	35190	0.33	5.52	**2392**
CH_2Cl_2	0.218	65.87	434	490	40200	0.42	6.21	**2633**
THF	0.208	66.18	432	488	41520	0.44	6.34	**2657**
n-Heptane	**0.0002**	**67.75**	**422**	**487**	**39020**	**0.49**	**6.61**	**3163**

Table 2. Spectral data of compound no. 2 in different solvents

Solvent	Δf	E_T (30) Kcal mol^{-1}	λ_{ab}(nm)	λ_{em}(nm)	ε M^{-1}cm^{-1}	f	μ Debye	$\Delta\bar{\nu}$ (cm^{-1})
DMF	0.275	73.87	387	456	24000	0.37	5.54	**3910**
MeOH	0.309	74.84	382	434	26300	0.27	4.69	**2594**
PrOH	0.280	74.84	382	430	26010	0.30	4.96	**2923**
ButOH	0.264	74.84	382	456	27400	0.46	6.13	**4249**
CH_2Cl_2	0.218	74.26	385	430	30190	0.32	5.17	**2719**
THF	0.208	75.43	379	445	26650	0.37	5.47	**3503**
n-Heptane	**0.0002**	**77.27**	**370**	**430**	**25090**	**0.33**	**5.16**	**3340**

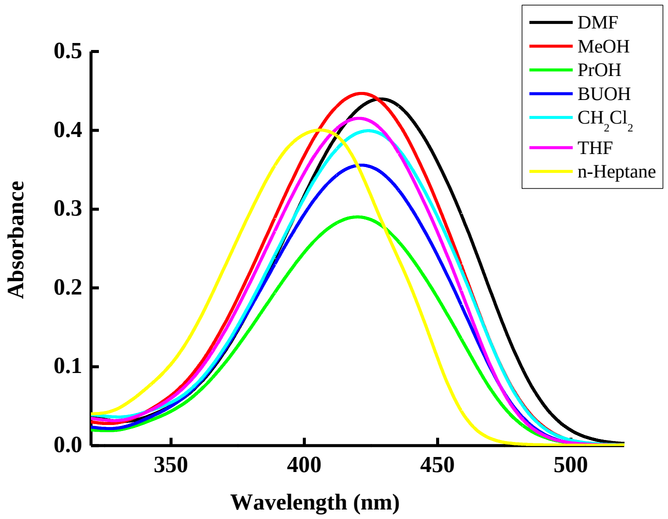

Figure 1a. Electronic absorption spectra of 1 × 10^{-5} mol dm^{-3} of compound **1** in different solvents

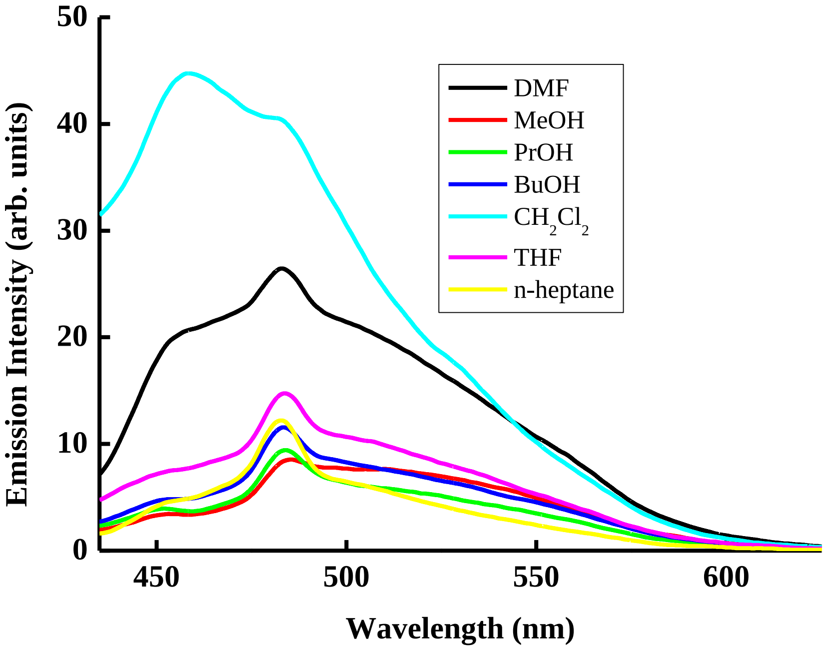

Figure 1b. Emission spectra of 1 × 10^{-5} mol dm^{-3} of compound **1** in different solvents

Table 3. Spectral data of compound no. 3 in different solvents

Solvent	Δf	E_T (30) Kcal mol^{-1}	λ_{ab}(nm)	λ_{em}(nm)	ε $M^{-1}cm^{-1}$	*f*	μ Debye	$\Delta\bar{\nu}$ (cm^{-1})
DMF	0.275	67.59	423	469	22880	0.21	4.35	2319
MeOH	0.309	68.89	415	467	24570	0.26	4.81	2683
PrOH	0.280	68.56	417	468	22850	0.24	4.69	2729
ButOH	0.264	68.23	419	468	22550	0.23	4.56	2613
CH_2Cl_2	0.218	68.39	418	472	22660	0.24	4.62	2680
THF	0.208	68.39	418	468	22490	0.22	4.50	2556
n-Heptane	0.0002	69.73	410	468	21630	0.26	4.76	3023

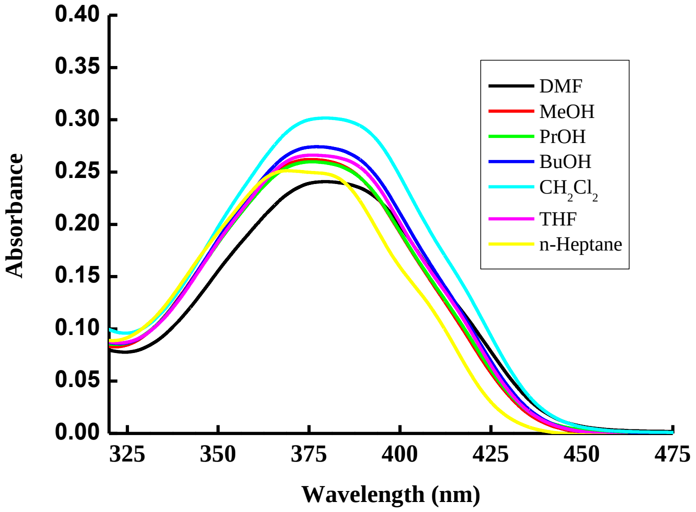

Figure 2a. Electronic absorption spectra of 1 × 10^{-5} mol dm^{-3} of compound **2** in different solvents

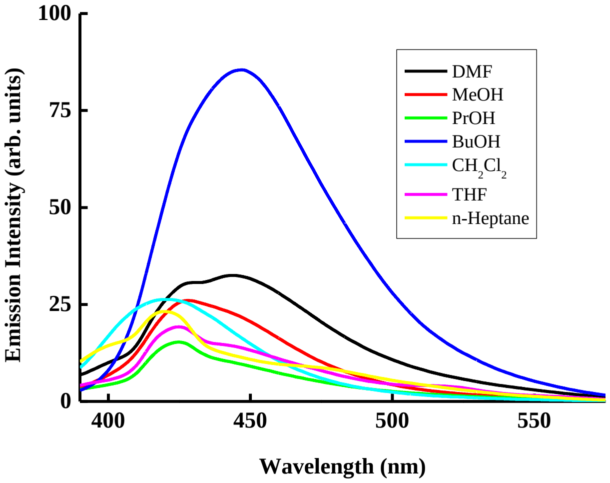

Figure 2b. Emission spectra of 1 × 10^{-5} mol dm^{-3} of compound **2** in different solvents

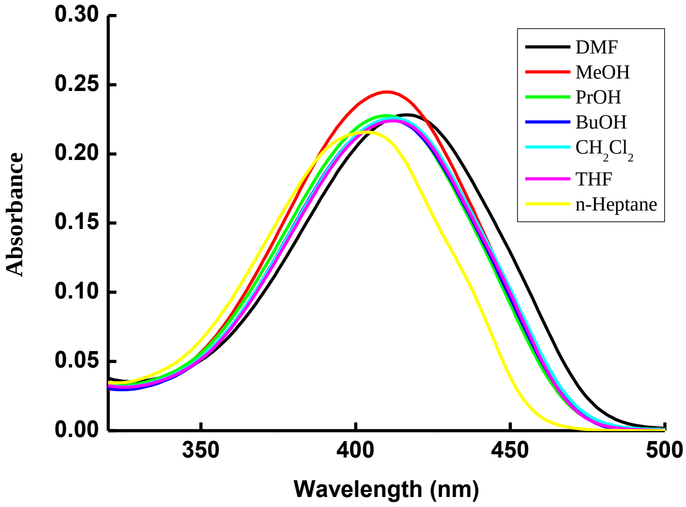

Figure 3a. Electronic absorption spectra of 1 × 10^{-5} mol dm^{-3} of compound **3** in different solvents

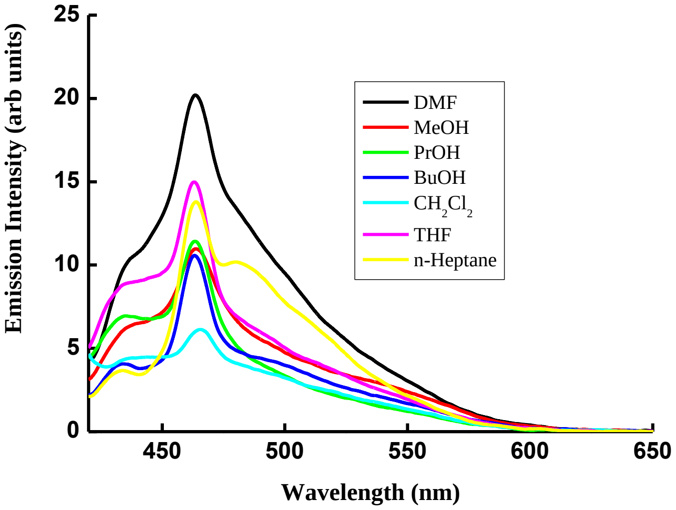

Figure 3b. Emission spectra of 1 × 10^{-5} mol dm^{-3} of compound **3** in different solvents

3.3. Determination of oscillator strength and transition dipole moment

The solvatochromic behavior in compounds (1-3) allows one to determine the difference in the dipole moment between the excited singlet and the ground state ($\Delta\mu = \mu_e - \mu_g$). This difference can be obtained using the simplified Lippert- Mataga equation as follows [29, 30]:

$$\Delta\bar{\nu}_{st} = \frac{2(\mu_e - \mu_g)^2}{hca^3}\Delta f + Const. \qquad (1)$$

$$\Delta f = \frac{D-1}{2D+1} - \frac{n^2-1}{2n^2+1} \qquad (2)$$

where $\Delta\bar{\nu}_{st}$ is the Stokes–shift [31], which increases with increasing the solvent polarity pointing to stronger stabilization of the excited state in polar solvents, *h* denotes Planck's constant, *c* refers to the speed of light in vacuum and *a* is the Onsager cavity radius. Parameters *D* and *n*, in equation 2, correspond to the dielectric constant and refractive index of the solvent, respectively. The Onsager cavity radius was chosen to be 4.2 Å because this value is comparable to the radius of a typical aromatic fluorophore [32]. Stokes shifts ($\Delta\bar{\nu}_{ss}$) of compounds (1-3) in different solvents were calculated, as shown in Table (1-3), using the following the equation [29]:

$$\Delta\bar{\nu}_{ss} = \bar{\nu}_{ex} - \bar{\nu}_{em} \qquad (3)$$

where $\bar{\nu}_{ex}$ and $\bar{\nu}_{em}$ denote the wavenumbers of excitation and emission maxima (cm^{-1}), respectively. The change in dipole moment (Δμ) for compound numbers 1, 2 and 3 are negative values of -4.66, -1.52 and -3.24 for respectively, which indicates that the ground state of these compounds is more polar than the singlet excited state.

The dimensionless microscopic solvent polarity parameters, E_T, can be obtained from equation (4) :

$$E_T(\text{kcal mol}^{-1}) = \frac{28591}{\lambda_{\max}(nm)} \qquad (4)$$

where $\lambda_{\max}$ is the wavelength of peak in the red region of the intramolecular charge transfer absorption of compounds (1-3).

The effective number of electrons transition from the ground to excited state is usually described by the oscillator strength, which provides the absorption area in the electronic spectrum. The oscillator strength, *f*, can be calculated using the following equation [33]:

$$f = 4.32 \times 10^{-9} \int \varepsilon(\bar{\nu})\, d\bar{\nu} \qquad (5)$$

where ε is the extinction coefficient ($\mathrm{Lmol^{-1}cm^{-1}}$), and $\bar{\nu}$ represents the numerical value of wavenumber ($\mathrm{cm^{-1}}$). Oscillator strength values of compounds (1-3) in different solvents are reported in Table 1-3. In addition, the transition dipole moment (μ) for compounds (1-3) from ground to excited state in Debye was estimated in different solvents (Table 1-3) using the following relation [34]:

$$\mu^2 = \frac{f}{4.72 \times 10^{-7} \times E_{\max}} \qquad (6)$$

where $E_{\max}$ is the maximum energy of absorption in $\mathrm{cm^{-1}}$

3.4. X-ray crystallographic Studies

The details of crystallographic parameters, information of data collection and structure refinements are given in Table 4. The particular bond lengths bond angles and dihedral angles are provided in Tables 5-7 respectively and are in accordance with already reported structures by our laboratory [35-38]. The three molecules differ in substitutions at various positions of only aromatic rings.

Table 4. Parameters for data collection and structure refinement of **1-3**

	1	**2**	**3**
Chemical Formula	$C_{18}H_{19}N_3S$	$C_{17}H_{16}N_2OS$	$\mathbf{C_{19}H_{20}N_2O_3S}$
M_r	309.42	296.38	**356.43**
Cell setting, space group	Orthorhombic, Pca 21	Monoclinic, $P2_1/c$	**Triclinic,** **P -1**
Temperature, K	296	296	**296**
A (Å)	16.319(2)	8.5487(1)	**8.5203(5)**
B (Å)	6.1075(7)	16.2740(2)	**10.3440(8)**
c (Å)	16.1703(2)	11.1517(2)	**12.0266(8)**
α (°)	90.00	90.00	**110.59(13)**
β (°)	90.00	96.157(2)	**102.178(5)**
γ, (°)	90.00	90.00	**104.253(6)**
V ($Å^3$)	1611.7(3)	1542.49 (4)	**911.59 (11)**
Z	4	4	**2**
Radiation; λ, Å	CuKα; 1.54180	CuKα; 1.54184	**CuKα; 1.54184**
D_x ($\mathrm{Mg\ m^{-3}}$)	1.275	1.276	**1.299**
μ ($\mathrm{mm^{-1}}$)	1.767	1.856	**1.744**
F000	658.89	624	**376**
Crystal form, colour	needles, yellow	block, yellow	**rod, yellow**

Crystal size (mm)	0.34 × 0.12 × 0.07	0.25 × 0.10 × 0.06	**0.45 × 0.18 × 0.15**
No. of measured, independent and observed reflections	3785, 2356, 2088	8936, 2718, 2363	**6943, 3584, 2684**
Criterion for observed reflection	$I > 2\sigma(I)$	$I > 2\sigma(I)$	**$I > 2\sigma(I)$**
R_{int}	0.0387	0.016	**0.0294**
θ_{max}, deg	74.23	66.58	**67.50**
$R[F^2 > 2\sigma(F^2)]$, $wR(F^2)$, S	0.087, 0.2271, 1.076	0.053, 0.1561, 1.07	**0.0546, 0.1613, 1.046**
No. of reflections	2356	2718	**3584**
No. of parameters	201	192	**229**
$(\Delta/\sigma)_{max}$	0.000	0.001	**0.001**
$\Delta\rho_{max}$, $\Delta\rho_{min}$ (eÅ^{-3})	0.518, -0.336	0.233, -0.332	**0.36, -0.33**

Table 5. Some selected bond lengths (Å) of the optimized geometry of 1-3 which were obtained by using DFT/B3LYP/6-31G(d) level of theory compared to its crystal structures

Parameter	I	Crystal	II	Crystal	III	Crystal
C5-C6	1.509	1.497	1.509	1.502	1.509	1.502
C1-C6	1.366	1.357	1.367	1.353	1.367	1.351
C1-C2	1.504	1.502	1.504	1.506	1.504	1.498
C1-S	1.753	1.726	1.752	1.724	1.753	1.726
C8-S	1.780	1.765	1.778	1.733	1.778	1.736
C8-N2	1.360	1.379	1.362	1.384	1.360	1.384
C9-N2	1.293	1.283	1.291	1.275	1.294	1.275
C7-C16	1.423	1.423	1.424	1.413	1.423	1.423
C16-N1	1.165	1.138	1.165	1.143	1.165	1.143
C9-C10	1.446	1.452	1.425	1.448	1.448	1.447
C10-C15	1.410	1.378	1.413	1.389	1.414	1.397

Table 6. Some selected bond angles (degrees) of the optimized geometry of 1-3 which were obtained by using DFT/B3LYP/6-31G(d) level of theory compared to its crystal structures

Parameter	I	Crystal	II	Crystal	III	Crystal
C6-C1-C2	125.3	124.0	125.2	124.8	125.3	125.3
C6-C1-S	112.2	112.4	112.3	112.4	112.3	112.5
C1-S-C8	91.6	92.2	91.6	91.9	91.6	91.9
C8-N2-C9	123.0	118.9	123.1	120.2	123.0	118.4
N2-C9-C10	122.9	124.2	122.5	123.1	121.5	123.1

C15-C10-C11	117.7	117.5	118.4	118.3	118.6	118.7

Table 7. Some selected dihedral angles (degrees) of the optimized geometry of 1-3 which were obtained by using DFT/B3LYP/6-31G(d) level of theory compared to its crystal structures

Parameter	I	Crystal	II	Crystal	III	Crystal
C6-C1-C2-C3	-15.3	-2.4	-15.5	-11.5	-15.4	-11.7
C6-C5-C4-C3	45.5	12.8	45.3	38.4	45.5	25.9
S-C1-C6-C7	-0.25	0.6	-0.24	-0.5	-0.25	0.5
C1-S-C8-N2	-179.9	179.0	179.9	179.0	-179.9	-177.3
C8-N2-C9-C10	-179.9	179.3	-179.9	-179.9	179.9	176.7
C9-C10-C11-C15	179.9	179.7	179.9	179.6	179.9	177.8

Molecule 1 ($C_{18}H_{19}N_3S$) contains *N*,*N*-dimethyl at the para position, molecule 2 ($C_{17}H_{16}N_2OS$) has a methoxy group while in molecule 3 ($C_{19}H_{20}N_2O_3S$) the 2nd, 4th & 5th positions are occupied by methoxy groups. The *ORTEP* diagrams are shown in Figures 4-7.

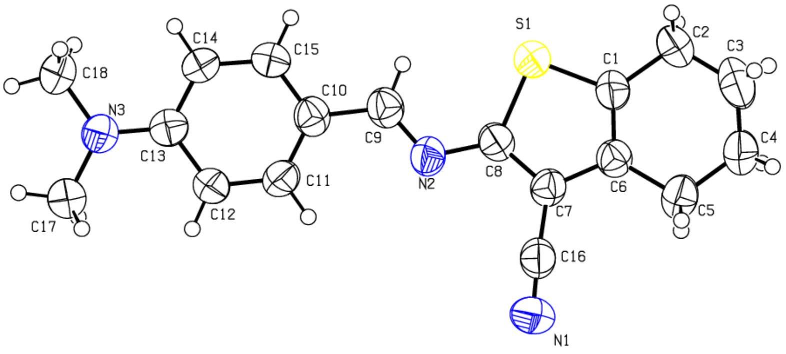

Figure 4. Labeled *ORTEP* diagram of Molecule 1 drawn with 50% probability level of thermal ellipsoids

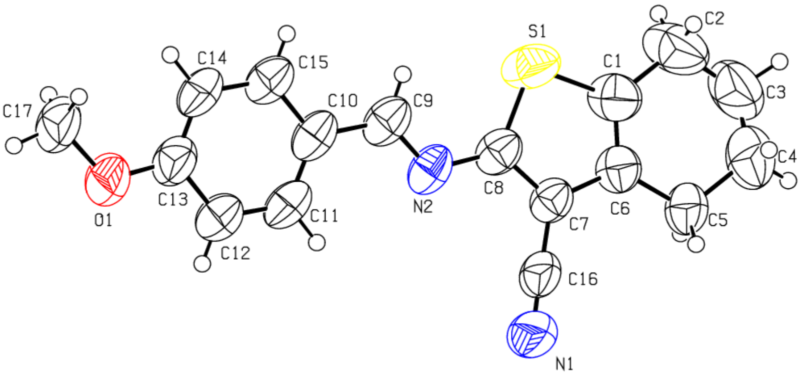

Figure 5. Labeled *ORTEP* diagram of Molecule 2 drawn with 50% probability level of thermal ellipsoids

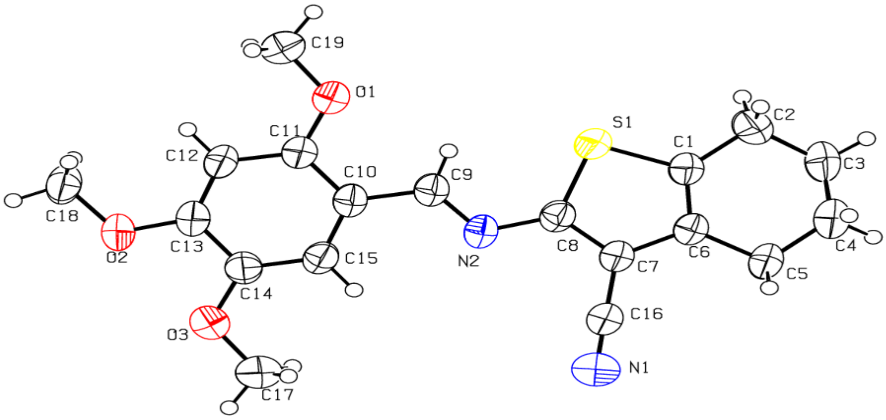

Figure 6. Labeled *ORTEP* diagram of Molecule 3 drawn with 50% probability level of thermal ellipsoids

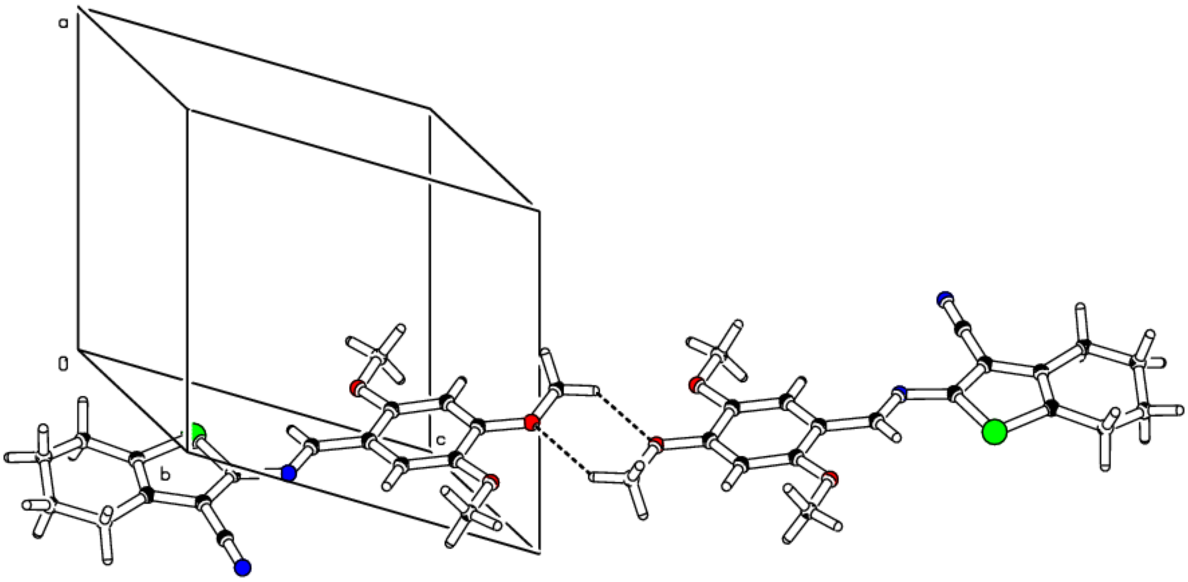

Figure 7. A unit cell view of molecule 3 showing the formation of inversion dimers

Table 8. Observed root mean square (r. m. s.) deviations of different moieties in molecules 1-3

Moiety	Molecule 1	Molecule 2	Molecule 3
Cyclohexene	0.0472(6)Å	0.1596(2)Å	0.1238(2)Å
Thiophene ring	0.0061(3)Å	0.0055(1)Å	0.0020(1)Å
Fused ring motif	0.0402(4)Å	0.1359(2)Å	0.1118(2)Å
Overall molecule	0.098(5)Å	0.1191(5)Å	0.1792(5)Å

Table 9. Observed dihedral angles between the planes formed through the joined atoms different moieties in molecules **1-3**

Moiety 1	Moiety 2	Molecule 1	Molecule 2	Molecule 3
Cyclohexene (C1-C6)	Thiophene	1.31(4)°	4.49(2)°	5.64(2)°
Cyclohexene (C1-C6)	Phenyl ring	6.76(4)°	10.13(1)°	13.64(2)°
Thiophene	Phenyl ring	7.72(3)°	6.26(1)°	8.03(1)°
Fused rings (C1-C8/S1)	Phenyl ring	7.05(3)°	9.15(1)°	11.25(2)°

Table 10. Non-classical hydrogen bonding interactions in molecules **3**

D---H	A	d(D---H) Å	d(H…A) Å	d(D…A) Å	<(D---H...A) (°)	Symmetry code
C18---H18B	O2	0.96	2.59	3.328(4)	134.3	1-X, 3-Y, 2-Z

Each molecule is composed of two fused rings i.e. cyclohexene, thiophene and a third aromatic ring. The root mean square (r.m.s) deviation values of fitted non-hydrogen atoms of each molecule are 0.098(5)Å, 0.1191(5)Å and 0.1792(5)Å respectively which describe that molecule 1 is slightly more planar than 2 and 3. The r.m.s deviations of cyclohexene, thiophene and these fused ring systems are given in table 5, which describe that the molecule 1 is almost planar while the cyclohexene ring in 2 has greater deviation from planarity of its fitted atoms and 3 has greater non-planarity than the other two. The tetrahydrobenzothiophene moiety (two fused rings) is twisted by about 7.05 (3) °, 9.15 (1) ° and 11.25 (2) ° with respect to the aromatic rings in molecules 1-3 respectively. The dihedral angles of planes generated through the atoms of different cyclic moieties are summarized in Table 9. The molecule 1 exhibits lowest dihedral angles and 3 the highest. The puckering parameters for the planes defined by atoms of cyclohexne are Q = 0.1157 (2) Å, θ = 51.81(3)° and φ = 152.45(2)° for (1), Q = 0.3910 (1) Å, θ = 128.32(2)° and φ = 329.08 (6)° for (2) and Q = 0.304 (3) Å, θ = 126.11(2)° and φ = 314.90(9)° for (3), respectively [39]. There is no classical hydrogen bonding nor C-H…π interactions observed in any of three molecules while the structure 2 is stabilized by a non-classical C---H…O interaction and generates inversion dimers by forming six membered ring motifs $R_2^2(6)$ table 10 [40].

3.5. Optimized geometry and electronic structure

In order to understand more about the structures of three molecules we performed density functional theory (DFT) studies (Fig. 8-10) [41]. There exists a remarkable agreement between the theoretical and experimental geometrical structures despite the fact that they are of different phases i.e.

the former is a gas-phase sample while the latter is a solid-phase crystal. This is perhaps due to the rigidity of the gas-phase structure as a result of the strong π-bonding character that resides more or less over the whole three molecules. The three molecules are perfectly planar apart from the non-planarity created around the methyl groups. The bond lengths and angles of the three rings and around them are nearly equal, apart from the N2-C9-C10 angles which open up by ca. 2.9^o – 4.5^o due to its floppy nature in the gas-phase for a moiety that connects two bulky groups. The differences between the dihedral angles of the theoretical and experimental structures reflect their different states but they both confirm the planarity of the three molecules.

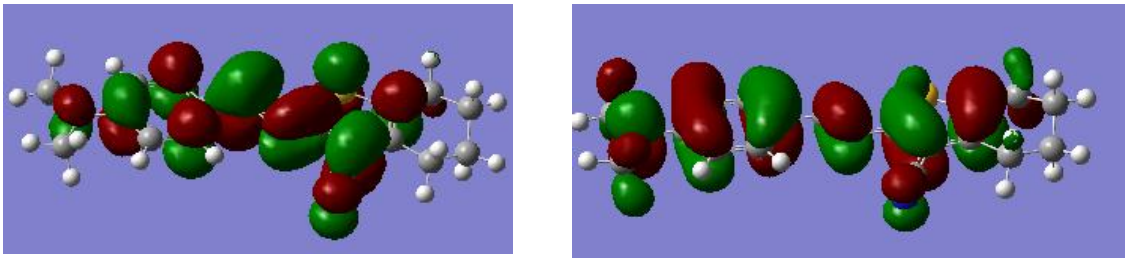

LUMO = -0.06889 a.u. HOMO = -0.18693 a.u.

Figure 8. The HOMO and LUMO Surfaces of 2-[(4-Dimethylamino-benzylidene)-amino]-4,5,6,7-tetrahydrobenzo[b]thiophene-3-carbnitrile (I)

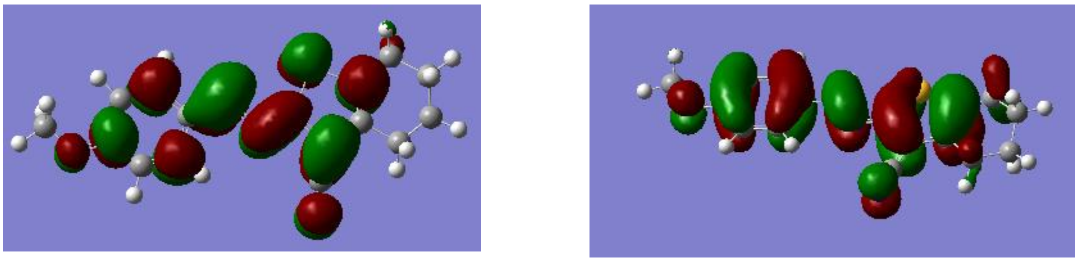

LUMO = -0.07725 a.u. HOMO = -0.20220 a.u.

Figure 9. The HOMO and LUMO Surfaces of 2-[(4-Methoxy-benzylidene)-amino]-4,5,6,7-tetrahydrobenzo[b]thiophene-3-carbnitrile (II)

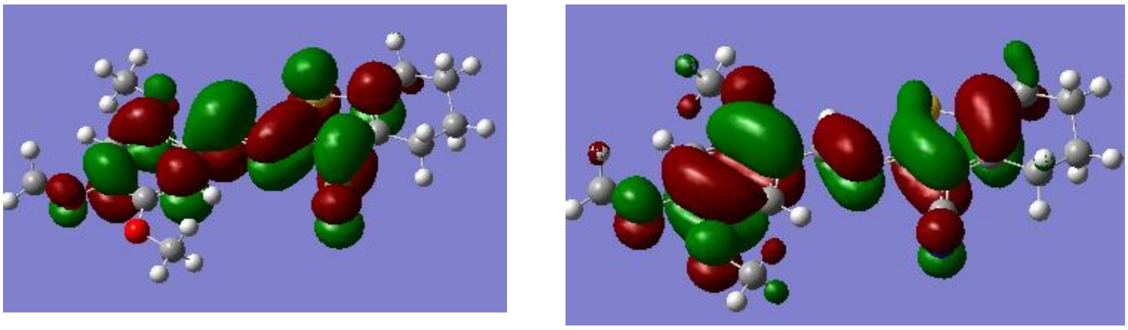

LUMO = -0.07107 a.u. HOMO = -.01882 a.u.

Figure 10. The HOMO and LUMO Surfaces of 2-[(2,4,5-trimethoxy-benzylidene)-amino]-4,5,6,7-tetrahydrobenzo[b]thiophene-3-carbnitrile (III)

3.6. Frontier molecular orbital energies

All HOMOs of I, II and III are mainly π-bonding molecular orbitals which are more or less located on the pentagonal and benzene rings and the C≡N and C=N bonds. Those of I and II are similar in this respect while that for III is characterized by strong π-bonding in the benzene ring towards the direction of the meta- and para- methoxy groups. This asymmetrical π-bonding has been reflected in unequal C-C bond lengths of the benzene ring. The LUMO of I, II and III are mainly of π-antibonding types that reside more or less over the pentagonal and benzene rings. They also have significant π-bonding characters over the C-C≡N, C-C=N and C=N-C moieties that connect the pentagonal and benzene rings. This fact has renders bonds around this region multiple bond characters and hence shorter than usual bond lengths. The HOMO of II is significantly lowered compared to I and III, respectively, which are nearly of the same energy. The LUMO of II is significantly lowered compared to I and III, respectively, which are nearly of the same energy. As a result, the energy gap (ΔE) of II is relatively greater than those for I and III by ca. 0.23 eV; while I and III have almost the same energy gaps, Table 11 [42].

Table 11. Electroic energies (a.u.), dipole moments (Debye), HOMO and LUMO energies (a.u.) and HOMO-LUMO energy gabs (ΔE/eV) of 1-3 which were obtained by using DFT/B3LYP/6-31G(d) level of theory compared to its crystal structures

Parameter	I	II	III
Electronic Energy	-1259.78655480	-1240.339604456	-1469.37874534
M	6.0368	5.9885	6.5222
HOMO	-0.18693	-0.2032	-0.1882
LUMO	-0.06889	-0.07725	-0.07107
ΔE	3.21	3.43	3.19

4. CONCLUSION

Three new azomethine dyes were synthesized with simple condensation method using 2-amino-4,5,6,7-tetrahydro-benzo[b]thiophene-3-carbonitrile and aldehydes variety. Physicochemical studies of these compounds including singlet absorption, extinction coefficient, Stokes shift, oscillator strength and dipole moment were investigated on the basis of the polarity of solvent. The synthesized compounds were characterized using spectroscopic techniques and further the structures were established using experimental technique i. e. single crysral diffraction studies. The DFT calculation was performed; molecular geometries and shapes were in good agreement with X-ray diffraction studies.

ACKNOWLEDGEMENT

This work was funded by the Deanship of Scientific Research (DSR), King Abdulaziz University, under grant No. (50-3-1432/HiCi). The authors, therefore, acknowledge technical and financial support of KAU.

References

1. A. M. Asiri, S. A. Khan, *Molecules,* 15 (2010) 6850-6858.
2. T. Taj, R. Kamble, T. Gireesh, B. Badami, *J. Chem. Sci.*, 123 (2011) 657-666.
3. M. Cacic, M. Trkovnik, F. Cacic, E. Has-Schon, *J. Hetrocy. Chem.*, 43 (2006) 261-266.
4. P. M. Ronad, M. N. Noolvi, S. Sapkal, S. Dharbhamulla, V. S. Maddi, *Eur. J. Med. Chem.,* 45 (2010) 85-89.
5. A. M. Asiri, S. A. Khan, *Molecules*, 15 (2010) 4784-4791.
6. R.C. Maurya, A. Pandey, J. Chaurasia, H. Martin, *J. Mol. Struct.*, 798 (2006) 89-101.
7. A. N. Kursunlu, E. Guler, F. Sevgi, B. Ozkalp, *J. Mol Struct.*, 1048 (2013) 476-481.
8. W. R. -Paryzek, V. Patroniak, J. Lisowski, *Coord. Chem. Rev.*, 249 (2005) 2156-2175.
9. N. S. Youssef, E. El-Zahany, A. M.A. El-Seidy, A. Caselli, S. Fantauzzi, S. Cenini, *Inorg. Chim. Acta*, 362 (2009) 2006-2014.
10. B. Pedras, L. Fernandes, E. Oliveira, L. Rodríguez, M. Manuela M. Raposo, J. L. Capelo, C. Lodeiro, *Inorg. Chem. Commun.*, 12 (2009) 79-85.
11. L. Mishra, S. K. Dubey, *Spectrochim. Acta, Part A,* 68 (2007) 364-368.
12. K. Bhat, K.J. Chang, M.D. Aggarwal, W.S. Wang, B.G. Penn, D.O. Frazier, *Mater. Chem. Phys.*, 44 (1996) 261-266.
13. G. Ceyhan, M. Tümer, M. Köse, V. McKee, S. Akar, *J Lumin.*, 132 (2012) 2917-2928.
14. A. –L. Brocas, C. Mantzaridis, D. Tunc, S. Carlotti, *Prog. Polym. Sci.*, 38 (2013) 845-853.
15. A. M. Asiri, S. A. Khan, H. M. Marwani, K. Sharma, *J. Photochem. Photobiol., B* 120 (2013) 82-89.
16. S.N. Pandeya, D. Sriram, G. Nath, E. DeClercq, *Eur. J. Pharma. Sci.,* 9 (1999) 25-31.
17. K. Sztanke, A. Maziarka, A. Osinka, M. Sztanke, *Bioorg. Med. Chem.*, 21 (2013) 3648-3666.
18. D. Sunil, A. M. Isloor, P. Shetty, P. G. Nayak, K.S.R. Pai, *Arabian J. Chem.*, 6 (2013) 25-33.
19. S. A. Khan, A. M. Asiri, A. A. Basheike, K. Sharma, *Eur. J. Chem.,* 4 (2013) 454-458.
20. S. A. Khan, A. M. Asiri, K. A. Khan, A. A. P. Khan, M. A. M. Zayed, *Asian J. Chem.,* 25 (2013) 8643-8646.
21. Agilent CrysAlis PRO. Agilent Technologies, Yarnton, England. 2012.
22. L.J. Barbour, X-Seed, *J. Supramol. Chem.*, 1 (2001) 189-191.
23. G.M. Sheldrick, Acta Cryst., 64 A (2008) 112-122.
24. A.L. Spek, *Acta Cryst*., D65 (2009) 148-155.
25. L.J. Farrugia, *J. Appl. Cr yst.,* 45 (2012) 849-854.
26. Spartan'04 Version 1.0.3, Wavefunction, Inc., Irvine
27. H. M. Marwani, A. M. Asiri, S. A. Khan, *Russ. J. Bioorgan. Chem.*, 38 (2012) 533-538
28. H. M. Asiri, A. M. Asiri, S. A. Khan. *J. Lumin.*, 136 (2013) 296-302
29. E. Lippert, *Z Electrochem.*, 61 (1957) 962-975
30. S. A. Khan, M. A. N. Razivi, A.H. Bakry, S. M. Afzal, A. M. Asiri, S. A. El-Daly, *Spectrochimica Acta A:* 137 (2015) 1100-1105.
31. S. A. Khan, A. M. Asiri, S. H. Al-Thaqafy, H. M.Faidallah, S. A. El-Daly, *Spectrochimica Acta A:* 133 (2014) 141-148.
32. S. Kumar, V. C. Rao, R. C. Rastogi, *Spectrochim. Acta A.* 57 (2001) 41-47.
33. N. J. Turro, Molecular photochemistry (frontiers in chemestry), 1st ed., W. A. Benjamin, Inc., Reading, MA, (1965) 286.
34. A.M. Asiri, S. A. Khan, M. S. Al-Amodi, K. A. Alamry. *Bull. Korean. Chem. Soc.* 33(2012) 1900-1906.
35. A.M. Asiri, S.A. Khan, M.N. Tahir, *Acta Cryst.*, E67 (2011) 02254.
36. A.M. Asiri, S.A. Khan, M.N. Tahir, *Acta Cryst.*, E67 (2011) 02355.
37. A.M. Asiri, S.A. Khan, M.N. Tahir, *Acta Cryst.*, E67 (2011) 02162.
38. H. Zhu, J. Zhu,L. Bu, J. Shi, J. Wanga, Acta Cryst., E68 (2012) 01368-01369.

39. D. Cremer , J. A. Pople, *J. Am. Chem. Soc.*, 97 (1975) 1354–1358
40. J. Bernstein, R. E. Davis, L. Shimoni, N. L. Chang, Patterns in Hydrogen Bonding: Functionality and Graph Set Analysis in Crystals Angew. Chem. Int. Ed. Engl. 34 (1995) 1555-1573.
41. S. A. Khan, A. M. Asiri, K. Sharma, *Med. Chem. Res.*, 22 (2013) 1998-2004.
42. S. A. Khan, A. M. Asiri, S. Kumar, K. Sharma, *Eur. J. Chem.*, 5 (2014) 85-90